

# Parametrization of the increase of the aeolian erosion threshold wind friction velocity due to soil moisture for arid and semi-arid areas

F. Fécan, B. Marticorena and G. Bergametti

LISA, Laboratoire Interuniversitaire des Systèmes Atmosphériques, Universités Paris 7-Paris 12, UMR CNRS 7583, Centre Multidisciplinaire de Créteil, 61 avenue du Général de Gaulle, F-94010 Créteil Cedex, France

Received: 6 February 1998 / Revised: 11 May 1998 / Accepted: 25 May 1998

**Abstract.** Large-scale simulation of the soil-derived dust emission in semi-arid regions needs to account for the influence of the soil moisture on the wind erosion threshold. Soil water retention consists of molecular adsorption on the soil grain surface and capillary forces between the grain. Interparticle capillary forces (characterized by the moisture tension) are the main factor responsible for the increase of the wind erosion threshold observed when the soil moisture increases. When the soil moisture content is close to but smaller than the maximum amount of adsorbed water,  $w'$  (depending on the soil texture), these capillary forces are considered as not strong enough to significantly increase the erosion threshold. An expression of the moisture tension as a function of soil moisture and  $w'$  is derived from retention curves. From this expression, a parametrization of the ratio of the wet to dry erosion thresholds has been developed as a function of soil moisture and soil texture. The coefficients of this parametrization have been determined by using experimental data from the literature. An empirical relationship between  $w'$  and soil clay content has been established. The erosion threshold ratios simulated for different soil textures were found to be in good agreement with the experimental data.

**Key words.** Atmospheric composition and structure (Aerosols and particles), Hydrology (soil moisture)

---

## 1 Introduction

Wind erosion in arid and semi-arid regions is the major source of tropospheric aerosols (Andreae, 1994). During transport in the atmosphere, these soil-derived particles strongly affect the radiative budget by backscattering and absorbing incoming (visible) and outgoing (infrared) radiation (Andreae, 1996; Li *et al.*, 1996). Moreover, recent works (Tegen *et al.*, 1996; Andreae, 1996)

suggest that dust emissions in semi-arid regions could increase due to human or climatic disturbances like overgrazing or drought. These changes in dust emissions from the semi-arid areas may significantly affect the radiative budget in the sub-tropical regions and, hence, the atmospheric global circulation (Li *et al.*, 1996).

Aeolian erosion occurs only when a threshold value of the wind velocity is reached and this threshold depends on the soil surface features. As a result, dust emissions are sporadic and spatially heterogeneous, making difficult any precise assessment of their impacts. Thus modelling is one of the best approaches to quantify dust emissions over arid and semi-arid areas.

A dust emission model representing the influence of the wind velocity and soil surface features has been developed for large-scale application (Marticorena and Bergametti, 1995; Marticorena *et al.*, 1997a). It includes a physical parametrization of the threshold friction velocity (the key parameter of the erosion processes) based on a drag partition scheme (in which the wind energy is transferred to the erodible surface as a function of the surface roughness length) and the size of the erodible aggregates. This parametrization has been validated with various experimental data obtained in wind tunnels (Marticorena and Bergametti, 1995; Marticorena *et al.*, 1997b). Applied to arid deserts, this model leads to satisfying spatial and temporal estimations of the soil-derived dust emissions (Marticorena and Bergametti, 1996; Marticorena *et al.*, 1997a). Precise estimations of dust emissions from these semi-arid areas required to complete this model developed with parametrizations that account for the influence of seasonal precipitation on the erosion thresholds. Precipitation has mainly two effects: (1) it allows the growth of seasonal vegetation able to absorb a part of the wind energy; and (2) soil moisture increases the erosion threshold due to reinforcement of soil cohesion.

The aim of the present work is to develop a parametrization of the influence of the soil moisture on the erosion threshold for large-scale simulations of dust emissions. This parametrization should involve

parameters available on such scales and should apply to most of the soils encountered in semi-arid areas. The influence of the seasonal vegetation will be investigated in a forthcoming paper.

## 2 Wet soil cohesion and wind erosion threshold

Chepil (1956) considered that the influence of soil moisture on wind erosion rates depends on soil texture and can be explained by interparticle cohesion forces due to soil water retention processes. Based on this work, a large number of relations has been proposed in order to link the erosion threshold to the soil moisture (Belly, 1964; Saleh and Fryrear, 1995; Shao *et al.*, 1996; Chen *et al.*, 1996). They consist mainly of numerical adjustments of the measured erosion threshold as a function of the soil moisture for a specific soil type (Belly, 1964; Shao *et al.*, 1996; Chen *et al.*, 1996) or for different types of soil (Saleh and Fryrear, 1996). In fact, such empirical parametrizations fail to reproduce other experimental data sets than those from which they have been established. In contrast, McKenna-Neuman and Nickling (1989) developed a parametrization of the increase of erosion threshold for sand based on a physical approach of the cohesion reinforcement of wet soils. After a brief examination of the physical processes involved in the reinforcement of the soil cohesion, we will extent this parametrization to other soil types.

For soil moisture lower than the field capacity, it is generally recognized (Hillel, 1980; Cornet, 1981) that the soil water (i.e. the liquid phase of the soil) is retained in the soil by two processes which interact with the soil matrix (i.e. the solid phase of the soil). Water wedges due to capillary forces are formed around the contact points of the grains and water films due to molecular adsorption appear on the grain surface. These mechanisms of soil water retention are generally combined in the “matric interactions”.

The capillary forces ( $F_c$ ) occurring in a wet soil were described by Fisher (1926) as the sum of (1) a difference of pressure  $\Delta p$ , inside and out of the water wedge, and (2) a tension force exerted by the air/water interface. The capillary forces are then expressed as follows:

$$\vec{F}_c = \Delta p \vec{S} + T \vec{\ell} \quad (1)$$

$\vec{F}_c$  : capillary force,

$\vec{S}$  : contact area ( $S = \pi R_2^2$ ),

$\vec{\ell}$  : perimeter of the contact zone ( $\ell = 2\pi R_2$ ),

$T$  : surface tension of water (0.072 Kg/s),

$\Delta p$  : pressure deficit between the inside and the outside of the water wedge,

$$\text{with } \Delta p = T \left( \frac{1}{R_1} - \frac{1}{R_2} \right) \quad (2)$$

$R_2$  : curvature radius of the waist of the water wedge depending on the soil moisture and grain shape,

$R_1$  : curvature radius of the air-water interface depending on the soil moisture and grain shape.

As the atmospheric pressure outside the water wedge is taken as a reference,  $\Delta p$  can be reduced to the pressure deficit  $P$  in the water wedge (Haines, 1925; Fisher, 1926; Hillel, 1980).

Haines (1925) and Fisher (1926) have applied Eqs. (1) and (2) to an ideal soil (i.e. spherical grains of uniform size) to explain the cohesion of wet soils (Fig. 1). The overall good agreement of their model with measurements of soil cohesion for various soil moistures underlines the major role played by the interparticle component of the capillary forces in the reinforcement of the soil cohesion. However, the hypothesis of spherical grains with uniform size limits the application of this model. Indeed, in such an ideal case, the relations between the curvature radii  $R_1$  and  $R_2$  and the soil moisture involve only the grain diameter, while in a real soil (i.e. with various shapes and grain sizes), the curvature radii depend strongly on the geometry of the grain contact areas. Hence, the application of this model to natural soils may lead to erroneous conclusions (Allberry, 1950).

The adsorption process is a complex phenomenon occurring at the interface between two phases. In the soil it occurs between the soil water and the soil matrix. Hillel (1980) indicates that the adsorption of water upon solid surface is generally of electrostatic nature. The polar water molecules attach themselves to the charged faces of the solid. The strength of the electrostatic attractive forces exerted on the water molecules (and consequently, the amount of water adsorbed at the surface of the grains) depends on the hygroscopic properties of the soil particles. The water adsorption around the grains is negligible for sands and increases with the soil clay content (Hillel, 1980). Very few studies deal with this adsorption film and its role in the wet soil cohesion.

However, Chepil (1956) and Chen *et al.* (1996) considered that the interparticle forces developed by

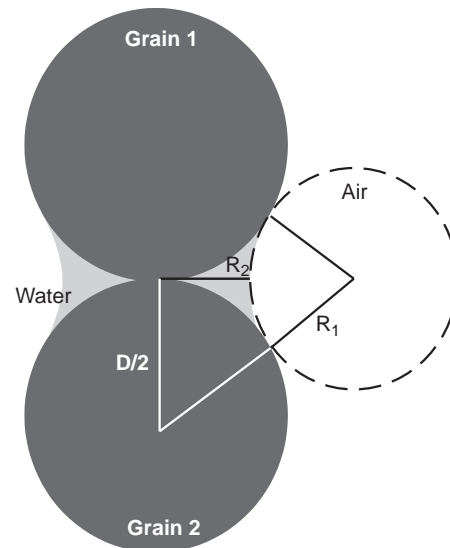


**Fig. 1.** Representation of the water wedge in an idealized soil (spherical grains of uniform size), adapted from Haines (1925)

the adsorbed water film are much lower than the interparticle capillary forces. This suggests that the reinforcement of the cohesion for wet soils is mainly due to the forces induced by the capillary effect, with a negligible influence of the adsorption film. Consequently, in terms of wind erosion, the increase of the threshold velocity with the soil moisture can be attributed in a large part to the interparticle component of the capillary forces.

Like Haines (1925) and Fisher (1926), McKenna-Neuman and Nickling (1989) based their model on a theoretical analysis of the interparticle capillary forces but they used a more realistic representation of the geometry of the contacts between grains. These authors considered that a reasonable approximation of the interparticle contact areas for natural grains is given by disymmetrical cones. Applying these geometric considerations to Eqs. (1) and (2) they described the interparticle capillary forces as a function of  $P$  and an adimensional geometric coefficient,  $G$ .  $G$  depends on the angles  $\alpha$  and  $\theta$  (see Fig. 2).

$$F_c = \frac{\pi T^2}{P} \cdot G \quad (3)$$

In contrast to Eqs. (1) and (2), this expression does not involve the curvature radii,  $R_1$  and  $R_2$ . Thus, the only parameter depending on the soil moisture is  $P$  (called moisture tension by the authors) which decreases when the soil moisture increases.

In order to describe the erosion threshold of wet soils, McKenna-Neuman and Nickling (1989) linked this capillary forces model to Bagnold's (1941) expression of the erosion threshold for dry soils. In fact, they

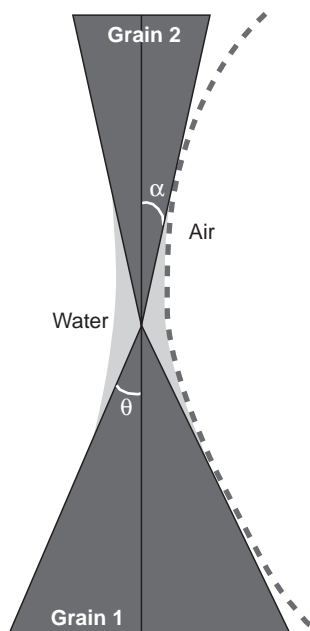


**Fig. 2.** Representation of the contact areas of the soil grain by disymmetrical cones, adapted from McKenna-Neuman and Nickling (1989)

simply considered erosion threshold friction velocity for moist particles ( $u_{*tw}$ ) as the product of the erosion threshold friction velocity for dry particles ( $u_{*td}$ ) by a term proportional to the square root of the capillary force. This term is:

for an open packed system:

$$\begin{aligned} \frac{u_{*tw}}{u_{*td}} &= \left[ 1 + \frac{F_c \cdot \sin(2\beta) \cdot \cos(\beta)}{\frac{\pi}{6} D^3 \cdot (\rho_p - \rho_a) g \cdot \sin(\beta)} \right]_{\beta=30^\circ}^{0.5} \\ &= \left[ 1 + \frac{T^2 \cdot G \cdot \sin(2\beta) \cdot \cos(\beta)}{\frac{1}{6} D^3 \cdot (\rho_p - \rho_a) g \cdot \sin(\beta) \cdot P} \right]_{\beta=30^\circ}^{0.5} \end{aligned} \quad (4)$$

for a close packed system:

$$\begin{aligned} \frac{u_{*tw}}{u_{*td}} &= \left[ 1 + \frac{F_c \cdot \sin(2\beta) \cdot (2\cos(\beta) + 1)}{\frac{\pi}{6} D^3 \cdot (\rho_p - \rho_a) g \cdot \sin(\beta)} \right]_{\beta=45^\circ}^{0.5} \\ &= \left[ 1 + \frac{T^2 \cdot G \cdot \sin(2\beta) \cdot (2\cos(\beta) + 1)}{\frac{1}{6} D^3 \cdot (\rho_p - \rho_a) g \cdot \sin(\beta) \cdot P} \right]_{\beta=45^\circ}^{0.5} \end{aligned} \quad (5)$$

- $D$ : mean grain diameter
- $\rho_p$ : grain density
- $\rho_a$ : air density
- $g$ : gravitational acceleration
- $\beta$ : particle resting angle
- $u_{*td}$ : dry erosion threshold friction velocity
- $u_{*td}$ : wet erosion threshold friction velocity

To test this parametrization, McKenna-Neuman and Nickling (1989) have performed wind tunnel experiments with three sands of different mean diameter (190  $\mu\text{m}$ , 270  $\mu\text{m}$ , 510  $\mu\text{m}$ ). They determined the moisture tension from the soil moisture, using experimental desorption curves, also called retention curves (Hillel, 1980). For the experimental range of moisture (0–2%), the thresholds computed by Eqs. (4) and (5) were found to be in good agreement with the measured thresholds (except for the highest soil moistures wherein the interparticle contacts coalesce). This suggests that the moisture tension would be the appropriate parameter to evaluate the wet threshold friction velocity.

However, McKenna-Neuman and Nickling (1989) underlined that, in its present state, their model cannot be applied to loam and clay soils.

### 3 Parametrization of the wind erosion thresholds of moist soils

Based on the described state-of-the-art knowledge two major conclusions can be drawn. First, the interparticle forces due to the adsorption film are much lower than the interparticle capillary forces. Secondly (and consequently), the base on which the McKenna-Neuman and Nickling's (1989) model is built can be used to develop a more general parametrization of the increase of thresholds for different types of wet soil.

### 3.1 Formulation of the parameterization of moist erosion thresholds

The parametrization developed by McKenna-Neuman and Nickling (1989) contains two types of variables: those describing the characteristics of the soil ( $G$ ,  $D$ ,  $\beta$ ,  $\rho_p$ ) and those characterizing the capillary forces due to the soil moisture ( $P$ ). Thus, Eqs. (4) and (5) can be expressed as follows:

$$\frac{u_{*tw}}{u_{*td}} = \left[ 1 + \frac{f(\text{soil properties})}{P} \right]^{0.5} \quad (6)$$

$u_{*td}, u_{*tw}$ : dry and wet erosion threshold friction velocities,

$P$ : moisture tension or capillary potential,

$f$ : function of the soil properties.

McKenna-Neuman and Nickling (1989) derived the moisture tension from experimental water retention curves by considering this tension as a direct function of the capillary forces. These experimental curves describe the water potential energy by unit of volume of the soil, generally called matric potential<sup>1</sup>, as a function of the soil moisture. Consequently, the matric potential represents all the interactions between the soil water and the soil matrix. Gardner (1970) proposed a well-recognized empirical relationship between the matric potential ( $\Psi$ ) and the soil moisture ( $w$ ):

$$\psi = aw^{-b} \quad (7)$$

$a, b$ : positive parameters depending on the soil type

$w$ : volumetric soil moisture

As mentioned already, the adsorption film is relatively unimportant for sand due to low molecular forces. In this case, the matric potential can be considered as an indicator of the strength of the capillary forces and can be considered as equal to the moisture tension as assumed by McKenna-Neuman and Nickling (1989). For other soils, a significant part of the soil moisture is trapped in the adsorption film due to the high molecular forces developed by the clay component of the soil. In this case, the matric potential includes not only the capillary forces but also the molecular adsorption forces. Consequently, it cannot be considered as equal to the moisture tension (Hillel, 1980).

Moreover, Hillel (1980) indicated that the capillary water and the adsorption film are in internal equilibrium. Owing to this equilibrium, Hillel (1980) argued that it was not possible to obtain a relation between the moisture tension and the matric potential. A possible alternative is to use a relationship similar to Eq. (7) to express the moisture tension  $P$ .

For a sand, as mentioned the soil moisture is mainly composed of capillary water since the adsorption is negligible ( $w \approx w_{\text{capillary}}$ ). In this case, the matric potential roughly equals the moisture tension ( $\Psi \approx P$ ). Thus,

Eq. (7) induces the following relationship between the moisture tension and the capillary moisture:

$$P = aw_{\text{capillary}}^{-b} \quad (8)$$

$a, b$ : Gardner's coefficients for sandy soils

For any other type of soil, the total moisture  $w$ , held back in the soil, is divided between a soil moisture responsible for capillary forces  $w_{\text{capillary}}$  and a soil moisture  $w_{\text{adsorbed}}$ , included only in the adsorption film:

$$w = w_{\text{capillary}} + w_{\text{adsorbed}} \quad (9)$$

Assuming that the moisture tension for a non-sandy soil can be formally expressed in the same manner as for sand, and considering Eq. (9), a general expression of the moisture tension  $P$  as a function of the soil moisture content is:

$$P = a'w_{\text{capillary}}^{-b'} = a'(w - w_{\text{adsorbed}})^{-b'} \quad (10)$$

By combining Eqs. (6) and (10), we obtain an expression of the erosion threshold ratio as a function of the soil moisture:

$$\frac{u_{*tw}}{u_{*td}} = \left[ 1 + A(w - w_{\text{adsorbed}})^{b'} \right]^{0.5} \quad (11)$$

with  $A = f(\text{soil properties})/a'$

According to the hypothesis sustaining Eq. (11), some dependence between the soil properties (geometry, soil type...) of the coefficients  $A$ ,  $b'$  and  $w_{\text{adsorbed}}$  can be expected.

Since Eq. (10) connects the moisture tension to the capillary water and not the matric potential to the soil moisture as in Gardner's retention curves, the coefficients  $a'$  and  $b'$  differ from  $a$  and  $b$  in Eq. (7). Consequently, it is difficult to presume on their dependence on the soil type.

For the coefficient  $A$ , the situation is clearer since it includes a description of the grain contact geometry.  $A$  at least, should depend on the soil structure.

Since the strength of the molecular adsorption forces depends on the soil clay content,  $w_{\text{adsorbed}}$  should increase with the soil clay content. Moreover, due to the equilibrium between capillary and adsorbed water,  $w_{\text{adsorbed}}$  should also depend on the total soil moisture ( $w$ ). In fact,  $w_{\text{adsorbed}}$  increases progressively with the total soil moisture until it reaches a limit, corresponding to the maximum amount of water that the adsorption molecular forces can trap (Hillel, 1980). However, there are no studies quantifying the variation and limit value of  $w_{\text{adsorbed}}$  as a function of the soil moisture. One possible approach consists in assuming that below a minimum soil moisture close to the limit value of  $w_{\text{adsorbed}}$  ( $w'$ ), the equilibrium is shifted toward the adsorbed water, and hence, the capillary moisture does not induce strong cohesion forces. This means that  $w'$  corresponds to the minimum soil moisture from which the threshold velocity increases. Considering  $w'$  close to the limit value of  $w_{\text{adsorbed}}$  implies that  $w'$  depends mainly on the soil clay content. Based on such an assumption, the parametrization can be expressed by:

<sup>1</sup> In fact, the retention curves rely the soil moisture to the matric suction which is the absolute value of the matric potential. Indeed, since the water is held back in the soil at a pressure below the atmospheric pressure taken as the reference, the matric potential is negative

$$\left. \begin{aligned} \frac{u_{*tw}}{u_{*td}} &= 1 && \text{for } w < w' \\ \frac{u_{*tw}}{u_{*td}} &= \left[ 1 + A(w - w')^b \right]^{0.5} && \text{for } w > w' \end{aligned} \right\} \quad (12)$$

The determination of  $A$ ,  $b'$  and  $w'$  can be based on measurements of the threshold for various soil moistures and for different soil texture. Their variation with the soil properties will be examined in relation with this discussion.

### 3.2 Empirical determination of $A$ , $b'$ and $w'$

The literature provides numerous wind tunnel measurements of wind erosion thresholds for many types of soil as a function of gravimetric soil moisture (Belly, 1964; Bisal and Hsieh, 1966; McKenna-Neuman and Nickling, 1989; Saleh and Fryrear, 1995; Chen *et al.*, 1996). However, these data have been obtained by using different experimental procedures which could lead to discrepancies in the results.

While soil moisture has always been determined by using an oven maintained at 105 °C, the determination of thresholds has involved various procedures. One of the major differences concerns the definition of threshold used. For Belly (1964), the erosion threshold is the point where the grain movement was fully sustained, whereas for most of the other authors, it corresponds to the initiation of the grain movement. Such a difference would lead to an overestimation of the thresholds measured by Belly (1964).

Secondly, in some experiments the wind profile is not determined since the wind velocity is only measured at one height. In these cases, the reported results are wind threshold velocity (Fig. 3), whereas in the other cases, the thresholds are expressed in term of threshold wind friction velocity (Fig. 4). To make both parameters comparable, the Prantl-Von Karman's relation can be used:

$$\frac{u_{*tw}}{u_{*td}} = \frac{u_{tw}(z)}{u_{td}(z)} \cdot \frac{\ln(z/z_{0d})}{\ln(z/z_{0w})} = \frac{u_{tw}(z)}{u_{td}(z)} \cdot K(z, z_{0d}, z_{0w}) \quad (13)$$

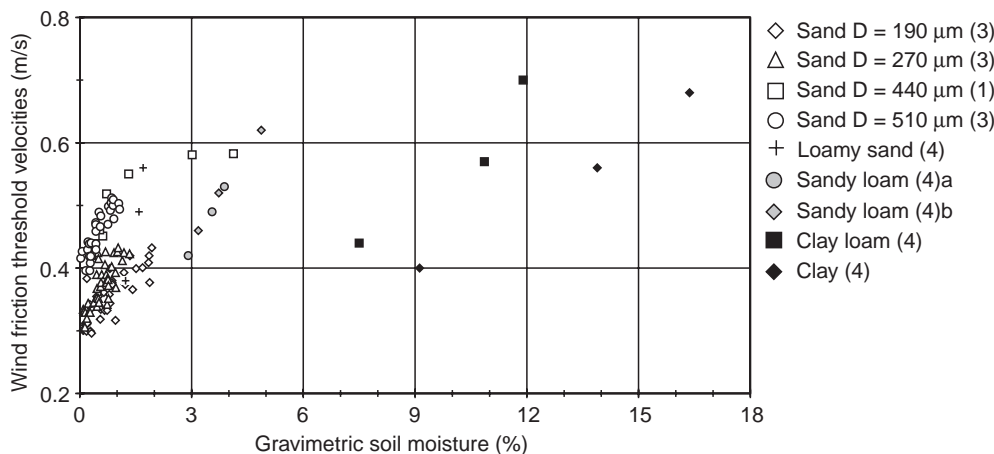


**Fig. 4.** Erosion threshold wind friction velocities ( $u_{*tw}$ ) as a function of the gravimetric soil moisture. Data from (1): Belly (1964); (3): McKenna-Neuman and Nickling (1989); (4): Saleh and Fryrear (1995)

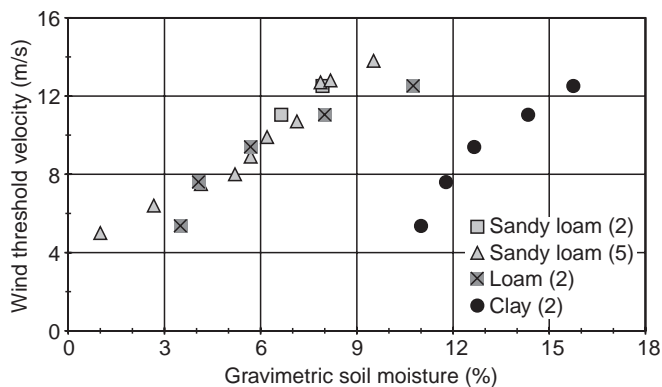


**Fig. 3.** Erosion threshold wind velocities ( $u_{tw}(z)$ ) as a function of the gravimetric soil moisture. Data from (2): Bisal and Hsieh (1966); (5): Chen *et al.* 1996)

- $u_{*tw}, u_{*td}$ : wet and dry threshold wind friction velocities
- $u_{tw}(z), u_{td}(z)$ : wet and dry threshold wind velocities at the height  $z$
- $z_{0d}, z_{0w}$ : surface roughness lengths of the dry and wet soils

The ratio of wet to dry threshold wind friction velocity ( $u_{*tw}/u_{*td}$ ) is proportional to the ratio of wet to dry threshold wind velocity ( $u_{tw}(z)/u_{td}(z)$ ), weighted by a coefficient  $K$  depending on the roughness lengths of the dry and wet soil. If the surface roughness length is not modified by the increase of the soil moisture, the two ratios can be considered as equal. To estimate the influence of a possible change of the surface roughness, the coefficient  $K$  was computed for various dry surface roughness lengths, assuming that the increase of the soil moisture has lead to a wet roughness length two times greater or lower than its initial dry value. For initial roughness lengths in the range of those measured on bare soils in wind tunnel (from  $10^{-2}$  to  $10^{-4}$  cm), the values of coefficient  $K$  always range between 0.9 and 1.1. This suggests that when the change in surface roughness length induced by the increase of the soil moisture is

neglected, an uncertainty of less than 10% is found in the ratio of wet to dry threshold wind friction velocity.

The measured threshold ratios  $u_{*w}/u_{*d}$  or  $u_{tw}(z)/u_{td}(z)$ , were plotted versus the gravimetric soil moisture ( $w$ ) for various types of soil (from sand to clay) (Fig. 5). The results clearly point to an increase in threshold ratios with  $w$  occurring at higher soil moisture when the soil clay content increases. A similar pattern is observed for the increase of the threshold ratio for various types of soil (except for the data obtained by Belly 1964 and by Saleh and Fryrear 1995 for a loamy sand). Despite the experimental limitations previously mentioned, these results show a great consistency over the various experimental data sets.

As a first step, we have adjusted Eq. (12) to the measured ratios for each soil to determine the value  $A$ ,  $b'$  and  $w'$  (Table 1).

The values obtained for  $A$ , and  $b'$  are more or less constant from one soil to another. Except for the outlier values obtained for Belly's (1964) data set (due to an overestimation of the measured thresholds) and for the loamy sand from Saleh and Fryrear's (1995) data set, mean values of  $1.3 \pm 0.2$ , and  $0.7 \pm 0.1$  are obtained

for  $A$  and  $b'$  respectively. These low standard deviations and the lack of clear trend of variation from one soil to another suggest that a constant value for  $A$  and  $b'$  could be used in a first approximation. However, the behaviour of  $w'$  is different: it increases continuously with the soil clay content (from 0 to about 12%). Thus, a second fit was performed, assuming that  $A$  and  $b'$  are constant for all soils,  $w'$  being the only term to vary according to the soil clay content. All sands were considered as one soil containing 0% clay.

The values resulting from this test are 1.21 and 0.68 for  $A$  and  $b'$  respectively, i.e. close to the mean values obtained in the former fit. Again,  $w'$  increases with the soil clay content, (Table 2) following a second order polynomial equation (Fig. 6).

$$w' = 0.0014(\% \text{clay})^2 + 0.17(\% \text{clay}) \quad (14)$$

The mean relative error induced by Eq. (14) is about 12%.

Finally, using the experimental data available in the literature, the coefficient  $A$  and  $b'$  were determined and found to be independent of the soil texture. A numerical relationship was established to retrieve  $w'$  from the soil

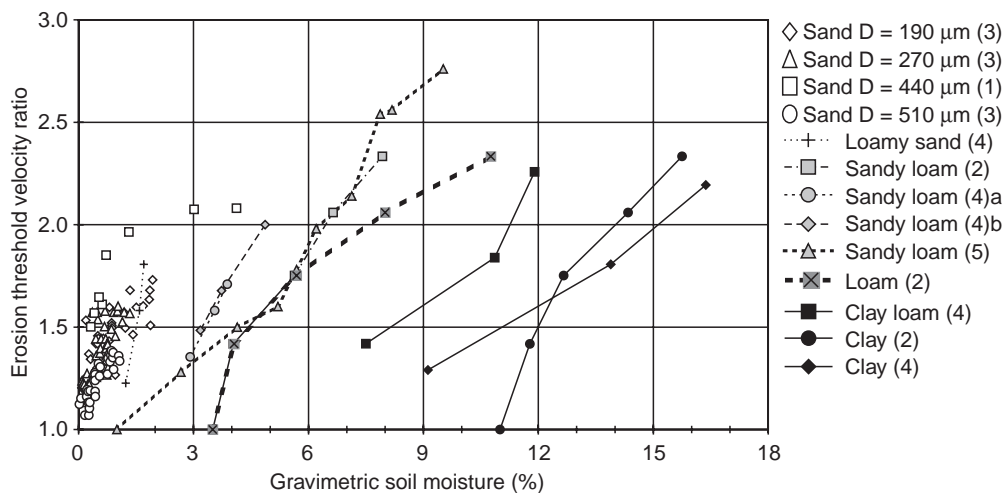


**Fig. 5.** Ratio of wet to dry threshold wind friction velocities or threshold wind velocities versus gravimetric soil moisture. Data from (1): Belly (1964); (2): Bisal and Hsieh (1966); (3): McKenna-Neuman and Nickling (1989); (4): Saleh and Fryrear (1995); (5): Chen *et al.* (1996)

**Table 1** Coefficients  $A$ ,  $b'$  and  $w'$  resulting from the fit of Eq. (12) to the measured erosion ratios for various soils. Data from (1): Belly (1964); (2): Bisal and Hsieh (1966); (3): McKenna-Neuman and Nickling (1989); (4): Saleh and Fryrear (1995); (5): Chen *et al.* (1996)

	% clay	$A$	$b'$	$w'$
Sand MD = 190 $\mu\text{m}^{(3)}$	0	1.27	0.45	0
Sand MD = 270 $\mu\text{m}^{(3)}$	0	1.22	0.64	0
Sand MD = 440 $\mu\text{m}^{(1)}$	0			0
Sand MD = 510 $\mu\text{m}^{(3)}$	0	0.87	0.59	0
Loamy sand <sup>(4)</sup>	8.5			1.01
Sandy loam <sup>(2)</sup>	9.2	1.52	0.67	3.5
Sandy loam <sup>(4)a</sup>	12.2	1.38	0.81	2.37
Sandy loam <sup>(4)b</sup>	14.2	1.42	0.81	2.37
Sandy loam <sup>(5)</sup>	–	1.28	0.77	3.3
Loam <sup>(2)</sup>	18.4	1.44	0.58	3.52
Clay loam <sup>(4)</sup>	31.6	1.55	0.55	7.15
Clay <sup>(2)</sup>	42.2	1.47	0.73	11.2
Clay <sup>(4)</sup>	49.2	1.07	0.62	8.8
Means		$1.3 \pm 0.2$	$0.7 \pm 0.1$	

**Table 2** Coefficients  $w'$  resulting from the fit of Eq. (12) to the measured erosion ratios for various soil clay content with  $A$  and  $b$  constant for all soils. Other results of this fit:  $b' = 0.68$  and  $A = 1.22$ . Literature data sets from (2): Bisal and Hsieh (1966); (3): McKenna-Neuman and Nickling (1989); (4): Saleh and Fryrear (1995); (5): Chen *et al.* (1996)

	% clay	$w'$
Sand <sup>(3)</sup>	0	0
Sandy loam <sup>(2)</sup>	9.2	3.5
Sandy loam <sup>(4)</sup>	12.2	2.3
Sandy loam <sup>(4)</sup>	14.2	2.11
Sandy loam <sup>(5)</sup>		
Loam <sup>(2)</sup>	18.4	3.5
Clay loam <sup>(4)</sup>	31.6	6.8
Clay <sup>(2)</sup>	42.2	11
Clay <sup>(4)</sup>	49.2	11.8

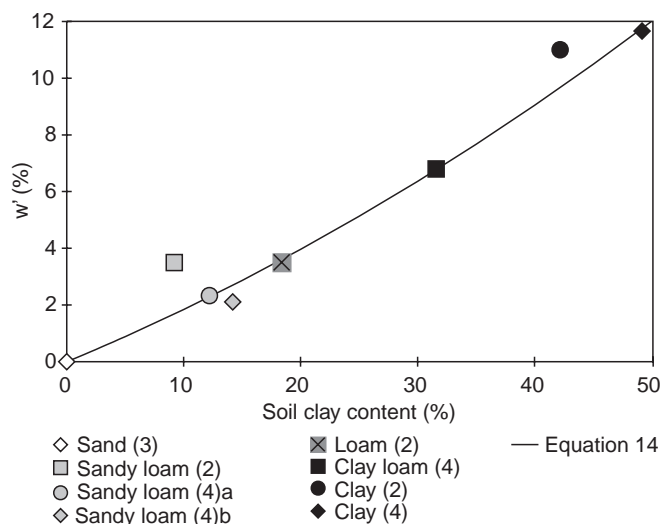


**Fig. 6.** Minimal soil moisture from which the wind erosion threshold increase ( $w'$ ) as a function of the soil clay content. Data from Table 2

clay content. An operational parametrization of the increase in the wind erosion thresholds as a function of the soil moisture is thus given by:

$$\left. \begin{aligned} \frac{u_{*tw}}{u_{*td}} &= 1 && \text{for } w < w' \\ \frac{u_{*tw}}{u_{*td}} &= \left[ 1 + 1.21(w - w')^{0.68} \right]^{0.5} && \text{for } w > w' \end{aligned} \right\} \quad (15)$$

with  $w' = 0.0014(\% \text{clay})^2 + 0.17(\% \text{clay})$

### 3.3 Validation

To evaluate the level of confidence of the developed parametrization, we have compared the threshold ratios computed from Eq. (15) to measured values (Fig. 7). Since  $w'$  is derived from the soil clay content, we used only the experimental data sets for which the soil clay content was determined. Moreover, in order to be consistent with the previous discussion, data from Belly

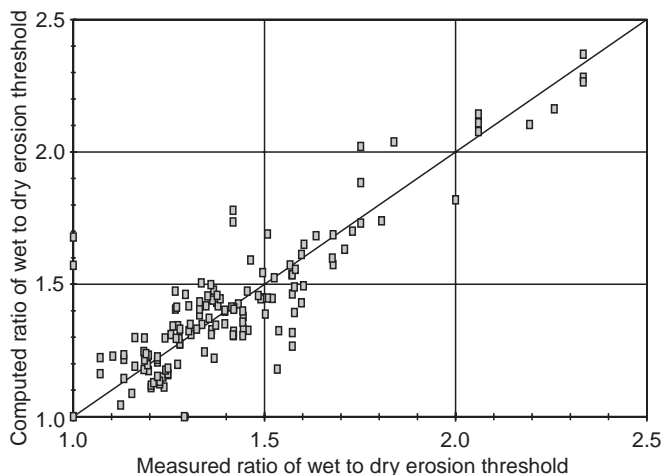


**Fig. 7.** Measured versus computed ratios of wet to dry erosion threshold (correlation coefficient  $r^2 = 0.75$ , confidence level  $>99.9$ , number of data = 140)

(1964) and the loamy sand from Saleh and Fryrear (1996) were discarded.

Despite a slight scattering of the data, Eq. (15) satisfies the measured thresholds. The mean relative error is 6.8% and for about 83% of the data the relative error is lower than 10%. This agreement is well illustrated in Fig. 8, where the measured and computed ratios were plotted versus the gravimetric soil moisture for each tested soil. For each texture class, the general trend of increase of the erosion threshold observed for the experimental data is well reproduced by Eq. (15), as well as the shift in the minimal soil moisture for which the threshold ratio increases.

This comparison indicates that the developed parametrization allows us to reproduce the observed increase of the thresholds due to soil moisture for the different soil textures likely to be encountered in semi-arid areas.

## 4 Concluding remarks

The satisfactory agreement obtained between the computed and experimental threshold ratios enables us to discuss hereafter the physical meaning of the coefficients.

The coefficient  $A$  expresses the influence of the soil structure (grain size, shape of the grain contact, packing...) on the wind thresholds. For the three sands for which information on grain mean diameter was available (McKenna-Neuman and Nickling, 1989), coefficient  $A$  decreases slightly from a fine sand to a coarse sand. In a first approximation, we have considered it independent of the soil type. The good agreement observed between computed and measured threshold ratios indicates that such an approximation does not affect the results significantly. If coefficient  $A$  constitutes a potential indicator of the influence of soil organisation on thresholds, these results suggest that this influence is negligible compared to that of soil texture.

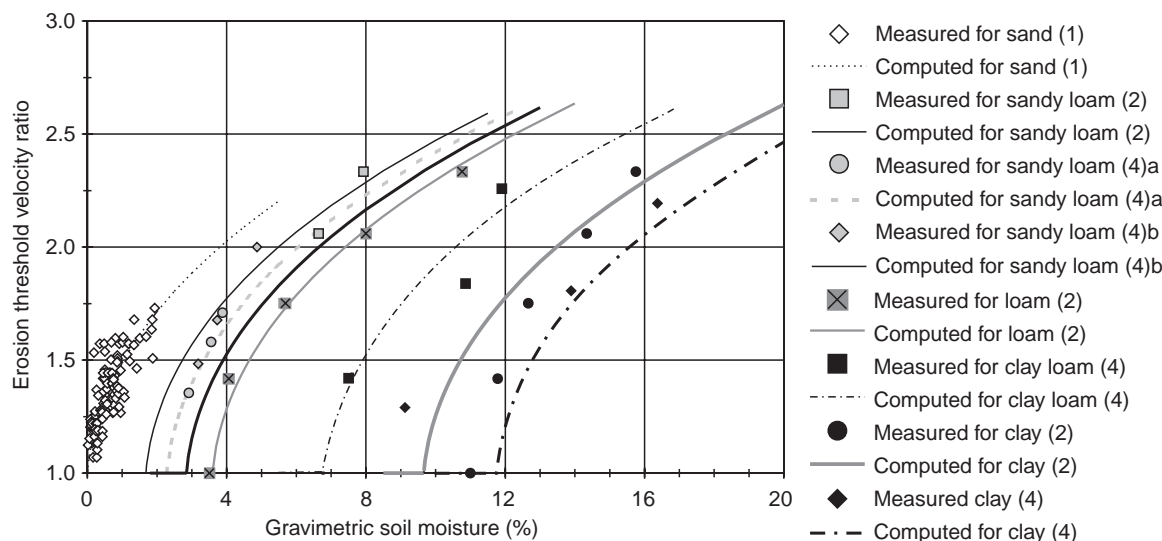


**Fig. 8.** Measured and computed erosion threshold ratio as a function of the gravimetric soil moisture. Data from (2): Bisal and Hsieh (1966); (3): McKenna-Neuman and Nickling (1989); (4): Saleh and Fryrear (1995)

The coefficient  $b'$  is one of the parameters linking the moisture tension to the soil moisture,  $w$ . It was found to be constant and equal to 0.68. This value corresponds to the coefficient  $b$  of Gardner's retention curves that can be estimated for sands (Mougin *et al.*, 1995; Cornet, 1981). This suggests that the soil moisture effect on the wind threshold can be considered identical for all soil textures and similar to that observed for sands, once the fraction of the soil moisture, which does not affect the reinforcement of the soil cohesion, has been subtracted.

We have defined  $w'$  as the minimal soil moisture required to induce an increase in threshold. From experimental data obtained for various soil types, this minimal moisture was found to increase with the soil clay content. The clayey component of the soil is known to influence the adsorption capacity of the soil, since it is responsible for electrostatic forces that maintain the water at the grain surface (Hillel, 1980). This suggests that  $w'$  is related to the maximum amount of water that can be retained in the soil by the adsorption films forming at the surface of the soil grains. Such a relation is thus consistent with the hypothesis of water separation in the soil sustaining our parametrization.

The limitations of this parametrization are linked to the main hypothesis on which it is based. The first one is that the capillary forces are responsible for threshold increases observed when the soil moisture increases and the adsorption processes do not induce significant interparticle cohesion forces. Secondly, due to the lack of a precise description of the water separation in the soil matrix, it was considered that, until a minimum soil moisture  $w'$  exists, close to the maximum adsorbed water amount, the capillary water induces negligible cohesion forces. This implies that below  $w'$ , the threshold is not influenced by an increase of the soil moisture and the ratio of wet to dry erosion thresholds remain constant and equal to 1. In fact, some authors have

observed a slight increase of the erosion threshold (Chen *et al.*, 1996) or a slight decrease of the erosion fluxes (Chepil, 1956) for soils with low moisture. They argued that the adsorption processes, dominant in this moisture range, produce low cohesion forces responsible for this progressive increase. Due to the equilibrium between the capillary and the adsorbed water, this increase may also be due to low capillary forces. A quantitative description of this equilibrium could enable a more precise simulation of the increase of the erosion thresholds for soils in the low soil moisture range.

Despite these limitations, the parametrization developed in this work fulfills the two main initial objectives of this study:

1. To describe the increase of the threshold for different soil textures with a satisfying confidence level.
2. To require only the soil moisture and the soil clay content as additional input parameters to those used in large-scale models of the mineral dust cycle. These two parameters are easily accessible at the considered scale. The soil moisture can be modelled from simple models of the soil water balance (precipitation-evaporation-evapotranspiration) as a function of meteorological parameters (precipitation rate, temperature, albedo) and on the soil type. The soil clay content, which controls the minimal soil moisture for the threshold increase, can be derived from texture maps (Zobler, 1980) that are generally used in the large-scale modelling of the mineral dust cycle.

*Acknowledgements.* This work was supported by the European Research Program « Environment and Climate » in the framework of the Project « MEDUSE ». The authors would like to thank M.V. Lopez, D. A. Gillette and C. Boissard for their comments on a draft of this paper.

Topical Editor J.-P. Duvel thanks two referees for their help in evaluating this paper.

## References

- Allberry, E. C., On the capillarity forces in an idealized soil, *J. Agric. Sci.*, **40**, 134–142, 1950.
- Andreae, M. O., Climate effect of changing atmospheric aerosol levels, in *World Survey of Climatology*, vol. XX. Future Climate of the World, Ed. A. Henderson-Sellers, 1994.
- Andreae, M. O., Raising dust in the greenhouse, *Nature*, **380**, 389–390, 1996.
- Bagnold, R. A., *The Physics of Blown Sand and Desert Dunes*, Methuen, London, 265 pp., 1941.
- Belly, P. Y., *Sand movement of wind*. TM Nol, US Army Coastal Engineering Research Center, Washington D.C., 80 pp., 1964.
- Bisal, F., and J. Hsieh, Influence of moisture on erodibility of soil by wind, *Soil Sci.*, **102**, 143–146, 1966.
- Chen, W., D. Zhibao, L. Zhenshan, and Y. Zuotao, Wind tunnel test of the influence of soil moisture on erodibility of loessial sandy loam soil by wind, *J. Arid Environ.*, **34**, 391–402, 1996.
- Chepil, W. S., Influence of moisture on erodibility of soil by wind, *Soil Sci. Soc. Am. Proc.*, **20**, 288–292, 1956.
- Cornet, A., Le bilan hydrique et son rôle dans la production de la strate herbacée de quelques phytocénoses sahéliennes au Sénégal, *Thèse Docteur Ingénieur*, Montpellier, 353 pp., 1981.
- Fisher, R. A., On the capillarity forces in an ideal soil; correction of formulae given by W. B. Haines, *J. Agric. Sci.*, **16**, 492–505, 1926.
- Gardner, W. R., Field measurement of soil water diffusivity, *Soil Sci. Soc. Am. Proc.*, **34**, 832–833, 1970.
- Haines, W. B., Studies of the physical properties of soils. II. A note on the cohesion developed by capillarity forces in an ideal soil, *J. Agric. Sci.*, **15**, 529–535, 1925.
- Hillel, D., *Fundamentals of soil physics*, Academic Press, New York, 1980.
- Li, X., H. Maring, D. Savoie, K. Voss, and J. M. Prospero, Dominance of mineral dust in aerosol light scattering in the North-Atlantic trade winds, *Nature*, **380**, 416–419, 1996.
- McKenna-Neuman, C., and W. G. Nickling, A theoretical and wind tunnel investigation of the effect of capillarity water on the entrainment of sediment by wind, *Can. J. Soil Sci.*, **69**, 79–96, 1989.
- Marticorena, B., and G. Bergametti, Modeling the atmospheric dust cycle: 1. Design of a soil-derived dust emission scheme, *J. Geophys. Res.*, **100**, 16, 415–16, 430, 1995.
- Marticorena, B., and G. Bergametti, Two year simulations of seasonal and interannual changes of the Saharan dust emissions, *Geophys. Res. Lett.*, **23**, 1921–1924, 1996.
- Marticorena, B., and G. Bergametti, B. Aumont, Y. Callot, C. N'Doume, and M. Legrand, Modeling the atmospheric dust cycle: 2. Simulation of the Saharan dust sources, *J. Geophys. Res.*, **102**, 4387–4404, 1997a.
- Marticorena, B., and G. Bergametti, D. A. Gillette, and J. Belnap, Factors controlling threshold friction velocity in semiarid and arid areas of the United States, *J. Geophys. Res.*, **102**, 23, 277–23, 287, 1997b.
- Mougin, E., D. Lo Seen, S. Rambal, A. Gaston, and P. Hiernaux, A regional Sahelian grassland model to be coupled with multi-spectral satellite data I: model description and validation, *Remote Sens. Environ.*, **52**, 181–193, 1995.
- Saleh, A., and D. W. Fryrear, Threshold wind velocities of wet soils as affected by wind blown sand, *Soil Sci.*, **160**, 304–309, 1995.
- Shao, Y., M. R. Raupach, and J. F. Leys, A model for predicting aeolian sand drift and dust entrainment on scales from paddock to region, *Aust. J. Soil Res.*, **34**, 309–342, 1996.
- Tegen I., A. A. Lacis, and I. Fung, The influence on climate forcing of mineral aerosols from disturbed soil, *Nature*, **380**, 419–422, 1996.
- Zobler, L., A world file for global climat modeling, *Tech. Rep. NASA-TM-87802*, 32 pp., 1986.